Comparative calculations of electron-swarm properties in N_2 at moderate E/N values

L. C. Pitchford* and A. V. Phelps†
Joint Institute for Laboratory Astrophysics, National Bureau of Standards and University of Colorado, Boulder, Colorado 80309

The recently developed density gradient and multiterm spherical harmonic expansion technique for the numerical solution of the electron Boltzmann equation is evaluated by comparison of results with those obtained using the conventional two-term spherical harmonic technique and using the Monte Carlo technique. Comparisons are made of electron energy distributions, transport coefficients, and excitation coefficients for electrons in N_2 at moderate electric-field to gas-density ratios E/N where the large cross section for vibrational excitation leads to significant errors when conventional solutions of the Boltzmann equation are used. The E/N values were varied from $(1-200)\times 10^{-21}$ V m^2, corresponding to mean electron energies from 0.3 to 5 eV. The first two terms of the density-gradient expansion are used. As the number of terms n in the spherical harmonic expansion is increased from the conventional two terms to $n \geq 4$, the spherically symmetric component of the electron energy distribution and the transport and excitation coefficients become independent of n and close to results obtained from the Monte Carlo calculation. The errors resulting from the use of two spherical harmonics at $E/N = 7\times 10^{-20}$ V m^2, for example, are approximately 1, 5, and 30% for the drift velocity, the transverse diffusion coefficient, and the electronic excitation coefficients, respectively. For the lower E/N values the errors in the transport coefficients are approximately proportional to an energy-loss-per-collision parameter. The variation of the coefficients of the lower-degree terms in the spherical-harmonic expansion with n is examined through a comparison with an analytical solution of the Boltzmann equation for a model atom valid in the case of low E/N and high electron energies. Monte Carlo techniques are used to show that the effects of electrodes are negligible for the conditions of recent measurements of electron excitation coefficients in N_2.

I. INTRODUCTION

In this paper we present a detailed discussion of the applicability of a technique recently developed by Pitchford, ONeil, and Rumble[1] (hereafter called I) to the calculation of energy distributions, transport coefficients, and excitation coefficients for electrons in N_2 at moderate values of E/N, the electric-field to gas-density ratio. We are especially interested in the errors introduced by the use of the commonly used two-term spherical harmonic expansion technique for a gas with cross sections which violate the assumptions of the technique. Nitrogen was chosen for this study because many authors[2–10] have used the two-term approximation even though the sum of the cross sections for vibrational excitation of N_2 is a large fraction of the elastic momentum transfer cross section.[4,11] A brief report by Long and Bailey[12] indicates that the convergence of a spherical harmonic expansion of the angular dependence of the electron energy distribution for N_2 is very slow at electron energies near the peak of the vibrational excitation cross section. In addition, Monte Carlo calculations of electron energy distributions for N_2 show large departures from spherical symmetry.[13] More recently, various authors[14–16] have calculated electron energy distributions and transport coefficients in other gases, e.g., CH_4 and CO, with large vibrational excitation cross sections and have found highly anisotropic electron distributions which are poorly represented by the two-term spherical harmonic expansion. The results presented in this paper for N_2 are expected to be representative of the results which would be obtained in other gases with large low-energy vibrational excitation cross

sections, e.g., CO, CO_2, CH_4, and SiH_4, or with large cross sections for rotational excitation, e.g., polar gases such as H_2O. We will show empirically that a decrease in the relative magnitudes of the terms of the spherical harmonic expansion is not a requirement for the convergence of the calculated transport and excitation coefficients to values independent of the number of terms in the expansion or for obtaining coefficients in agreement with values given by the Monte Carlo technique.

In I it was shown that the use of six terms in the spherical harmonic expansion resulted in a convergence of the calculated drift velocities and transverse diffusion coefficients for electrons in N_2. We will extend these results to include longitudinal diffusion coefficients and electron excitation coefficients and will examine the systematics of the errors resulting from the use of the conventional two-term spherical harmonic approximation. We will also make comparisons of the electron energy distributions and the transport and excitation coefficients with the results of Monte Carlo calculations. In particular, Sec. II contains a summary and comparison of the equations used to calculate the transport and rate coefficients in both the multiterm and two-term spherical harmonic approximations. In Sec. III numerical comparisons of the two-term and multiterm calculations are used to demonstrate the convergence of the results with increasing number of terms and show the correlation of the results with an electron energy loss parameter. Also, the multiterm calculations are compared with the Monte Carlo results. Section IV contains a simple technique for calculating the energy and angular dependence of the energy distribution at high energies and low E/N which illustrates the effect of changing the number of terms in the spherical harmonic expansion. In Sec. V Monte Carlo techniques are used to show that electrode effects cause negligible errors in the application of the calculated excitation coefficients to typical experiments in N_2.

II. THEORY OF CALCULATIONS

In this section we summarize the theoretical expressions actually used in the calculations to be presented in Sec. III. Since the general theory of the expansions in powers of the spatial gradients and in spherical harmonics has been given elsewhere,[1,17] we will keep only the terms used in the actual calculations.

The Boltzmann equation for electrons specifies the dependence of the electron distribution function $F(\vec{r},\vec{v},t)$ on position $\vec{r}$, velocity $\vec{v}$, and time t. It is written as

$$\frac{\partial F}{\partial t}+\vec{v}\cdot\vec{\nabla}_r F+\vec{a}\cdot\vec{\nabla}_v F=NC(F)\ , \tag{1}$$

where $\vec{a}=-|e/m|\vec{E}$ is the acceleration of the electron of charge e and mass m due to an external electric field, and C is the collision operator to be discussed later. In this paper we will neglect processes which result in the production or loss of electrons, i.e., attachment and ionization, so that $C(f)$ includes only the effects of elastic and inelastic or energy-loss collisions.

The distribution function of $F(\vec{r},\vec{v},t)$ can be written in terms of functions which depend only on $\vec{v}$ and a function which depends only on $\vec{r}$ and t by using the first two terms of an expansion in powers of the density gradients,[17,18] i.e.,

$$F(\vec{r},\vec{v},t)=f(\vec{v})n(\vec{r},t)-\frac{g_r(\vec{v})}{N}\frac{\partial n(\vec{r},t)}{\partial r}-\frac{g_z(\vec{v})}{N}\frac{\partial n(\vec{r},t)}{\partial z}\ . \tag{2}$$

Here $f(\vec{v})$, $g_r(\vec{v})$, and $g_z(\vec{v})$ are velocity distributions and $n(\vec{r},t)$ is the electron-density distribution. Substitution of Eq. (2) into Eq. (1) and integration over all velocities yields the continuity equation for electrons, i.e.,

$$\frac{\partial n(\vec{r},t)}{\partial t}=-w\frac{\partial n(\vec{r},t)}{\partial z}+D_L\frac{\partial^2 n(\vec{r},t)}{\partial z^2}+D_T\frac{1}{r}\frac{\partial}{\partial r}\left[r\frac{\partial}{\partial r}n(\vec{r},t)\right]\ , \tag{3}$$

where[17]

$$w=\int v\cos\theta f(\vec{v})d^3v\ , \tag{4}$$

$$D_L N=\int v\cos\theta g_z(\vec{v})d^3v\ , \tag{5}$$

$$D_T N=\int v\sin\theta g_r(\vec{v})d^3v\ , \tag{6}$$

and θ is the angle between the velocity vector and the direction $(+z)$ of acceleration of the electron due to the electric field. From the form of Eq. (3) w is identified as the electron-drift velocity and $D_T N$ and $D_L N$ are the transverse and longitudinal[18] components of the electron-diffusion tensor normalized to unit gas density. The approximation represented by Eq. (3) with its time- and space-independent coefficients is known as the hydrodynamic approximation.[17] Because of the absence of electron production and loss terms in $C(f)$ the

term proportional to $n(\vec{r},t)$ is missing from Eq. (3).

Equations for the velocity distributions $f(\vec{v})$ and the components of $\vec{g}(\vec{v})$ are obtained by substitution of Eq. (2) into Eq. (1) and setting coefficients of $n(\vec{r},t)$ and its various derivatives equal to zero.[17] The resultant equations are

$$\vec{a}\cdot\vec{\nabla}_v f(\vec{v})=NC[f(\vec{v})] , \tag{7}$$

$$\vec{a}\cdot\vec{\nabla}_v g_z(\vec{v})= NC[g_z(\vec{v})] -N(w-v\cos\theta)f(\vec{v}) , \tag{8}$$

and

$$\vec{a}\cdot\vec{\nabla}_v g_r(\vec{v})=NC[g_r(\vec{v})]+Nv\sin\theta f(\vec{v}) . \tag{9}$$

The utility of the expansion of $f(\vec{r},\vec{v},t)$ in powers of the gradient of $n(\vec{r},t)$, Eq. (2), is now apparent. Using this expansion, Eq. (1) has been transformed from one equation in $\vec{r}$, $\vec{v}$, and t into an equation in $\vec{r}$ and t, i.e., Eq. (3), and a set of equations in $\vec{v}$, i.e., Eqs. (7)–(9). Furthermore, Kumar *et al.*[17] show that Eqs. (4)–(9) are unchanged when additional terms are added to the density-gradient expansion given in Eq. (2). We next consider the solutions of Eqs. (7)–(9).

A. Multiterm spherical harmonic solution

As in I, Eq. (7) is solved by writing $f(\vec{v})$ as the sum of the first n terms of a spherical harmonic expansion in $\cos\theta$ which, because of the axial symmetry of the problem, becomes an expansion in zero-order Legendre polynomials $P_j(\cos\theta)$. Thus,

$$f(\vec{v})=\sum_{j=0}^{n-1} f_j(\epsilon)P_j(\cos\theta) , \tag{10}$$

where the normalization condition is

$$\int_0^\infty \epsilon^{1/2}f_0(\epsilon)d\epsilon=1$$

and $\epsilon=mv^2/2$ is the electron energy. Substitution of Eq. (10) into Eq. (7) leads to a set of n-coupled differential equations[19] of the form

$$\frac{eE}{N}\frac{j}{(2j-1)}\left[\epsilon\frac{df_{j-1}}{d\epsilon}-\frac{(j-1)}{2}f_{j-1}\right]+\frac{eE}{N}\frac{(j+1)}{(2j+3)}\left[\epsilon\frac{df_{j+1}}{d\epsilon}+\frac{(j+2)}{2}f_{j+1}\right]=C[f_j(\epsilon)] , \tag{11}$$

for $j=0,\ldots,(n-1)$. Since we neglect collisions of the second kind as well as collisions resulting in attachment and ionization, $C[f_j(\epsilon)]$ is given by

$$C[f_j(\epsilon)]=-\epsilon f_j(\epsilon)Q_T(\epsilon)+\epsilon f_j(\epsilon)Q_j^0(\epsilon) + \sum_{k=1}^{p}(\epsilon+\epsilon_k)f_j(\epsilon+\epsilon_k)Q_j^k(\epsilon+\epsilon_k) + \frac{2m}{M}\delta_{j0}\frac{d}{d\epsilon}[\epsilon^2 Q_m^s(\epsilon)f_j(\epsilon)] , \tag{12}$$

$$Q_j^k(\epsilon)=\int P_j(\cos\theta_s)I_k(\epsilon,\theta_s)d\Omega , \tag{13}$$

$$Q_m^s=\sum_{k=0}^{p}(Q_0^k-Q_1^k) ,$$

and

$$Q_T(\epsilon)=\sum_{k=0}^{p}Q_0^k(\epsilon) .$$

In Eq. (11) and the remainder of this paper $E=|\vec{E}|$. As in I the k index on the cross section Q_j^k designates elastic scattering for $k=0$ and the kth inelastic or energy-loss process for k from 1 to p, Q_T is the sum of the "total" scattering cross sections, Q_m^s is the sum of the momentum transfer cross sections $Q_0^k-Q_1^k$, $I_k(\epsilon,\theta_s)$ is the differential cross section for scattering of an electron into a solid angle $d\Omega$ and through an angle θ_s, and M is the mass of the N_2 molecule. The set of n equations given by Eq. (11) is solved for the $f_j(\epsilon)$ functions using the Galerkin method discussed in detail in I. Although a detailed analysis of boundary conditions was not carried out in I, they found that the representation of the $f_j(\epsilon)$ using sets of energy-dependent functions which are zero beyond some electron energy ϵ_{max} plus the normalization condition on $f_0(\epsilon)$ is sufficient to define the solutions to Eqs. (11). The results presented in this paper were obtained using these constraints[20] on the $f_j(\epsilon)$. The electron-drift velocity w can then be calculated by noting that substitution of Eq. (10) into Eq. (4) yields

$$w=\frac{1}{3}\left[\frac{2}{m}\right]^{1/2}\int_0^\infty \epsilon f_1(\epsilon)d\epsilon . \tag{14}$$

Equations (8) and (9) for $g_r(\vec{v})$ and $g_z(\vec{v})$ are solved using the same techniques as used for $f(\vec{v})$ and Eq. (7). Thus, $g_z(\vec{v})$ is also expanded in Legendre polynomials of zero order, i.e.,

$$g_z(\vec{v})=\sum_{j=0}^{n-1} G_j(\epsilon)P_j(\cos\theta) . \tag{15}$$

Substitution of Eq. (15) into Eq. (8) yields a set of n equations of the form

$$\frac{eE}{N}\frac{j}{(2j-1)}\left[\epsilon\frac{dG_{j-1}}{d\epsilon}-\frac{(j-1)}{2}G_{j-1}\right]+\frac{eE}{N}\frac{(j+1)}{(2j+3)}\left[\epsilon\frac{dG_{j+1}}{d\epsilon}+\frac{(j+2)}{2}G_{j+1}\right]$$
$$=C[G_j(\epsilon)]+\frac{j}{(2j-1)}\epsilon f_{j-1}-\left[\frac{\epsilon m}{2}\right]^{1/2} wf_j+\frac{(j+1)}{(2j+3)}\epsilon f_{j+1} , \tag{16}$$

for $j=0, \ldots, (n-1)$. Here $C[G_j(\epsilon)]$ is obtained by substituting $G_j(\epsilon)$ for $f_j(\epsilon)$ in Eq. (12). An additional equation results from the requirement[17] that the normalization integral for $g_z(\vec{v})$ will be zero or

$$\int_0^\infty \epsilon^{1/2}G_0(\epsilon)d\epsilon=0 .$$

Note that once the set of $f_j(\epsilon)$ functions have been obtained as described in I and w has been evaluated using Eq. (14), the last three terms of Eq. (16) are known. Equations (16) are then solved for the $G_j(\epsilon)$ functions with the same techniques and boundary conditions[21] used to obtain the $f_j(\epsilon)$ functions. The quantity D_LN is evaluated using Eq. (5) which reduces to

$$D_LN=\frac{1}{3}\left[\frac{2}{m}\right]^{1/2}\int_0^\infty \epsilon G_1(\epsilon)d\epsilon . \tag{17}$$

Symmetry considerations in the case of $g_r(\vec{v})$ require the use of an expansion of $g_r(\vec{v})$ in associated Legendre polynomials of the first kind. Thus,

$$g_r(\vec{v})=\sum_{j=1}^{n-1} H_j(\epsilon)P_j^1(\cos\theta) , \tag{18}$$

where the lower limit to the sum is $j=1$ because P_0^1 is not defined. Substitution of Eq. (18) into Eq. (9) yields $n-1$ equations[22] of the form

$$\frac{eE}{N}\frac{(j-1)}{(2j-1)}\left[\epsilon\frac{dH_{j-1}}{d\epsilon}-\frac{(j-1)}{2}H_{j-1}\right]+\frac{eE}{N}\frac{(j+2)}{(2j+3)}\left[\epsilon\frac{dH_{j+1}}{d\epsilon}+\frac{(j+2)}{2}H_{j+1}\right]$$
$$=C[H_j(\epsilon)]+\frac{1}{(2j-1)}\epsilon f_{j-1}-\frac{1}{(2j+3)}\epsilon f_{j+1} , \tag{19}$$

for $j=1, \ldots, (n-1)$. Here $C[H_j(\epsilon)]$ is evaluated by substitution of $H_j(\epsilon)$ for $f_j(\epsilon)$ in Eq. (12) and the $f_j(\epsilon)$ are known from the solution of Eqs. (11). Solutions of Eqs. (19) are obtained using the techniques and boundary conditions[21] of I. D_TN is evaluated using Eq. (6) which can be written as

$$D_TN=\frac{1}{3}\left[\frac{2}{m}\right]^{1/2}\int_0^\infty \epsilon H_1(\epsilon)d\epsilon . \tag{20}$$

The rate of excitation of N_2 to the rotational, vibrational, and electronic excited states ν_k is obtained by considering the portion of the collision term $C(f)$ of Eq. (12) representing the loss of electrons from an element of velocity space due to the kth inelastic process and integrating over velocity space. Thus, the excitation frequency for process k is given

$$\nu_k=N\int vI^k(v,\theta_s)f(\vec{v})d^3v$$
$$=N\left[\frac{2}{m}\right]^{1/2}\int_{\epsilon_k}^\infty \epsilon Q_0^k(\epsilon)f_0(\epsilon)d\epsilon . \tag{21}$$

In the case of steady-state drift-tube experiments,[23,24] the results are more naturally expressed in terms of the number of excitation events per unit distance in the direction of electron drift α_k, i.e., in terms of

$$\alpha_k=\nu_k/w . \tag{22}$$

We will use the terminology "n-term" expansion

or solution to indicate solutions to Eqs. (11), (16), and (19) obtained using j values up to $j=n-1$, e.g., a six-term expansion would be solutions to Eq. (11) using the first six spherical harmonics of Eq. (10).

B. Two-term spherical harmonic solution

In our calculations the two-term results, i.e., $n=2$, are obtained by simultaneously solving the $j=0$ and 1 equations of Eqs. (11), (15), and (19) with $f_2(\epsilon)$, $G_2(\epsilon)$, and $H_2(\epsilon)$ set equal to zero. Of particular importance in the discussion to follow is the fact that we retained the inelastic collision terms of Eq. (12) for $j=1$, as well as $j=0$. This procedure is in contrast to what we will term conventional two-term solution[2,3] in which the inelastic collision terms are assumed to be small enough so that they can be neglected compared to the elastic collision terms of Eq. (12) for $j=1$. Since the contribution of inelastic terms to $C[f_1(\epsilon)]$ is assumed negligible in the conventional two-term solution, the $j=1$ equation of Eqs. (11) becomes

$$-\frac{eE}{N}\frac{df_0}{d\epsilon}=[Q_0^0(\epsilon)-Q_1^0(\epsilon)]f_1(\epsilon)$$
$$\equiv Q_m^0(\epsilon)f_1(\epsilon)\ , \tag{23}$$

where $Q_m^0(\epsilon)$ is the elastic momentum transfer cross section. Substitution of Eq. (23) into Eq. (14) yields the usual equation for the evaluation of w and the closely related mobility $\mu\equiv w/E$. Thus,

$$w^{\mathrm{II}}=-\frac{eE}{3m}\left[\frac{2}{m}\right]^{1/2}\int_0^\infty \frac{\epsilon}{Q_m^0(\epsilon)}\frac{df_0(\epsilon)}{d\epsilon}d\epsilon\ .$$

As pointed out by Baraff and Buchsbaum,[25] most applications[4–10] of the conventional two-term approximation use an effective momentum transfer cross section which is obtained by fitting calculated and experimental electron transport data. This effective momentum transfer cross section may well include significant inelastic contributions. This procedure is justifiable, for example, in gases for which inelastic scattering is not negligible but is isotropic. In this case one can define an effective momentum transfer cross section $Q_m(\epsilon)$ in Eq. (23) which is equal to $Q_T(\epsilon)-Q_1^0(\epsilon)$. In our calculations, the additional assumption of isotropic elastic scattering means that $Q_m^s(\epsilon)=Q_T(\epsilon)$ except in the last term of Eq. (12), i.e., except in the elastic-recoil term.

The conventional two-term expression for the transverse diffusion coefficient follows from Eq. (19), when $n=2$ so that only the $j=1$ equation remains and $C[H_1(\epsilon)]=-\epsilon f_0$. When inelastic scattering is negligible or is included in an effective momentum transfer cross section this becomes $Q_m(\epsilon)H_1(\epsilon)=f_0(\epsilon)$ so that Eq. (20) becomes the conventional expression, i.e.,

$$D_T^{\mathrm{II}}=\frac{1}{3}\left[\frac{2}{m}\right]^{1/2}\int_0^\infty \frac{\epsilon f_0(\epsilon)d\epsilon}{Q_m(\epsilon)}\ . \tag{24}$$

Most of the conventional two-term calculations of electron transport and reaction coefficients[4,6–10] have calculated the lateral diffusion coefficient but have not calculated the longitudinal diffusion coefficient. In their calculations of D_LN for N_2 and other gases, Lowke and Parker[5] used the equivalent of the procedures of this paper for $n=2$, except that (a) the term proportional to $wf_1(\epsilon)$ was neglected in Eq. (16) in the case of $j=1$ and (b) they required $G_0(\epsilon)=0$ at $\epsilon=0$ rather than the integral condition on $G_0(\epsilon)$ given after Eqs. (16). Tagashira, Sakai, and Sakamoto[18] have reported that the $D_L^{\mathrm{II}}N$ values are independent of which condition is imposed on $G_0(\epsilon)$. We agree with them. In our notation the expression of Lowke and Parker[18] is

$$D_L^{\mathrm{II}}N=D_T^{\mathrm{II}}N-\frac{eE}{N}\left[\frac{2}{m}\right]^{1/2}\int_0^\infty \frac{\epsilon}{Q_m(\epsilon)}\frac{dG_0(\epsilon)}{d\epsilon}d\epsilon$$
$$-w^{\mathrm{II}}\int_0^\infty \epsilon^{1/2}G_0(\epsilon)d\epsilon\ . \tag{25}$$

Thus, even in the conventional two-term solution, the evaluation of D_LN requires the solution of Eqs. (16). Since the techniques of I used in this paper to solve Eqs. (16) with $n=2$ yield $G_1(\epsilon)$, as well as $G_0(\epsilon)$, we will use Eq. (17) to evaluate D_LN rather than Eq. (25).

C. Monte Carlo calculations

Monte Carlo calculations of energy distributions and transport and ionization coefficients for electrons in N_2 have been carried out using the computer program developed by Reid.[16] The cross-section set used was the same as that used for the Boltzmann calculations of Secs. II A and II B. The calculations of the drift velocities and the transverse diffusion coefficients were carried out by following a single electron for from 10^6 to 5×10^6 collisions. The simulations of electron excitation experiments were carried out using various fixed drift distances and a total of 10^6 collisions. The

electrons were injected in a direction normal to the electrodes and the electrodes were assumed to be completely absorbing.

III. NUMERICAL RESULTS

In this section we discuss the convergence of the distribution functions and the transport and rate coefficients calculated using the method discussed in Sec. II for the case of N_2 over a range of E/N from $(1-200)\times 10^{-21}$ V m^2. In this range of E/N in N_2 average electron energies go from near the vibrational thresholds, through the vibrational cross section maximum to near electronic thresholds, i.e., 0.3 to 5 eV. The cross-section set used for these calculations[24] is shown in Fig. 1. These cross sections are assumed to result in isotropic scattering. The momentum transfer cross section shown is therefore equal to the sum of the elastic and inelastic cross sections. The rotational-excitation cross sections,[4] for which an example is shown in Fig. 1, were replaced by an effective cross section for a single level.[26] The vibrational and electronic cross sections are shown in the figure as sums of the individual level excitations. In the calculation we used the individual level cross sections and, with ionization, included a total of 23 inelastic cross sections. The range of E/N was low enough that ionization could be treated as an energy-loss process. At the highest value of E/N used, 2×10^{-19} V m^2, only about 3% of the electron energy loss goes into ionization. For higher E/N, the fact that a second electron is produced in the ionization event begins to significantly affect the distribution and must be included as such.

Since the computational problem begins with the determination of the Legendre expansion coefficients, the $f_j(\epsilon)$'s, we will first look at those. The normalized $f_j(\epsilon)$'s in N_2 at an E/N of 10^{-19} V m^2 (where the average energy of the electrons in the swarm is 2.2 eV) are shown in Fig. 2 as a function of energy. The results shown are the first four coefficients in a six-term spherical harmonic expansion. The isotropic component $f_0(\epsilon)$ is the largest at all energies. The coefficients $f_j(\epsilon)$ for $j\geq 1$ become comparable with $f_0(\epsilon)$ at about 2 eV where the vibrational cross sections are large. The structure in $f_2(\epsilon)$ and $f_3(\epsilon)$ which occurs near 2 eV and again near 7 eV seems to be associated with the onset of important inelastic cross sections.

Application of the theory of Sec. II to the calculation of transport and rate coefficients requires that one calculate accurately only the first few coefficients $f_j(\epsilon)$ of the Legendre expansions. Because of the coupling among Eqs. (11), the solution obtained for $f_0(\epsilon)$, for example, will depend on the number of terms in the expansion. Figure 3 shows the results of calculations of $f_0(\epsilon)$ using a two-term expansion, a six-term expansion, and the Monte Carlo technique. The E/N is the same as in Fig. 2. The six-term solution and the Monte Carlo solution for $f_0(\epsilon)$ agree very well at all energies except those near the origin.[27] A four-term solution was also carried out for this E/N value and yielded an $f_0(\epsilon)$ very close to the six-term

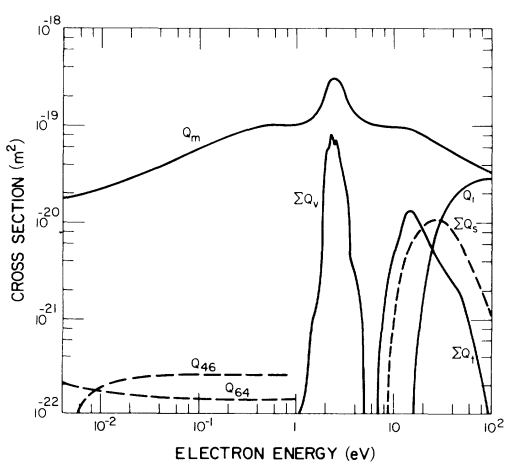

FIG. 1. N_2 cross sections used in the calculations of this paper. The excitation cross sections shown are sums over many of the 23 individual cross sections used.

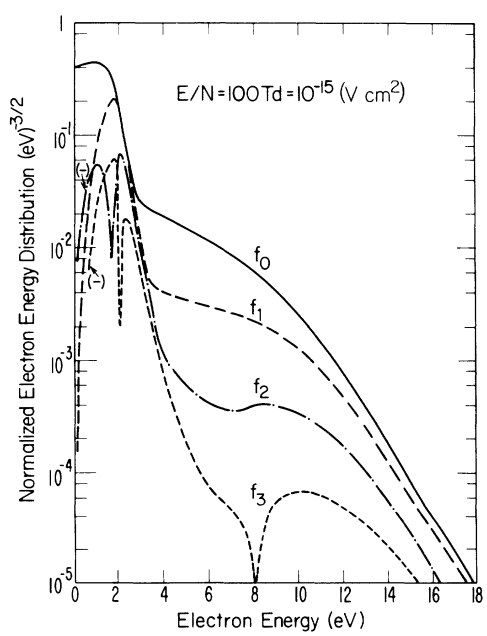

FIG. 2. The first four normalized Legendre coefficients of a six-term solution for the electron energy distribution function in N_2 at $E/N=10^{-19}$ V m^2.

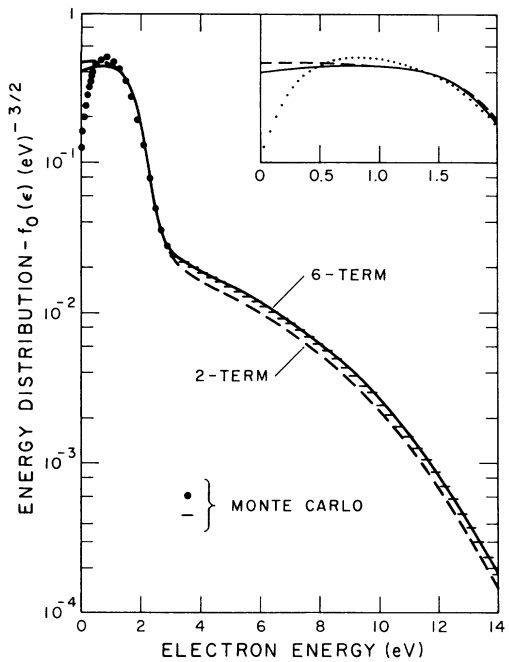

FIG. 3. Comparison of the normalized $f_0(\epsilon)$, the isotropic component of the distribution function, calculated using two- and six-term spherical harmonic expansion solutions to the Boltzmann equation and a Monte Carlo technique. The solid circles and bars are 0.05- and 0.3-eV averages, respectively, of a Monte Carlo calculation using 5×10^6 collisions.

solution. Since these energy distributions are obtained by two completely different methods, we conclude that with the possible exception of very low energies, the $f_0(\epsilon)$ calculated using the multiterm expansion converge very quickly to a function close to the correct solution even though the higher order $f_j(\epsilon)$ in Fig. 2 are still quite large. Of particular importance for the calculation of electronic excitation rate coefficients is the increase in the high-energy portion of $f_0(\epsilon)$ as n is increased.

The curves of Fig. 4 show the variation of the drift velocity, transverse and parallel diffusion coefficients, and the electronic excitation coefficient for the $N_2(A^3\Sigma)$ state in case of nitrogen at 10^{-19} V m^2 as a function of the number n of spherical harmonic components used in the calculation. The values of these coefficients and of the excitation coefficients for the $v=0\rightarrow1$ vibrational excitation of N_2 are given in Table I. From Fig. 4 it can be seen that the two-term values of the drift velocity and the transverse diffusion coefficient are larger than the values obtained using $n>2$. Conversely, the values of the A-state excitation coefficient, illustrative of electronic excitation in general,[28] and the parallel diffusion coefficients are lower for the two-term solution than for the $n>2$ calculations. The increase in the excitation coefficient for the A state is the result of the increase in $f_0(\epsilon)$ with n shown in Fig. 3. The decrease in D_T and the increase in D_L with increasing n are presumably the result of a more accurate calculation of the anisotropy of the electron energy distribution, i.e., the result of changes in $G_1(\epsilon)$ and $H_1(\epsilon)$ with increasing n. The calculated values are seen to converge as the number of terms in the spherical harmonic expansion is increased, i.e., beyond four terms there is very little change in the transport and excitation coefficients. The calculated vibrational excitation coefficients for the $v=0\rightarrow1$ transition listed in Table I decrease with increasing n. The results of the Monte Carlo calculation of the electron-drift velocity, the transverse diffusion coefficient and the $N_2(A^3\Sigma)$ excitation coefficient are shown in Fig. 4 by the dashed lines. For the drift velocity and the $A^3\Sigma$ excitation the differences between the spherical harmonic expansion values and the Monte Carlo results are within the estimated calculational uncertainties. The larger difference in the transverse diffusion coefficient calculated by the two techniques is not understood.[16]

Calculations similar to the one presented in Fig. 4 were carried out over a range of E/N from $(1-200)\times10^{-21}$ V m^2 and the difference between the two-term and six-term results are shown in Fig. 5 as a function of E/N. See also Table I. The convergence of the transport and excitation coefficients with increasing n for the seven values of E/N investigated is similar to that shown in Fig. 4. The differences between the values of the drift velocity and the transverse diffusion coefficient for the two-term calculation and those for the six-term result increase with increasing E/N to a maximum at 7×10^{-20} V m^2 and then decrease. Thus, the maximum errors occur when many of the electrons have energies for which the sum of the inelastic cross sections is a large fraction of the sum of the momentum transfer cross sections.[2,3] The largest errors in the electronic excitation coefficients occur at the lowest E/N.

It is of interest to compare the results of the conventional two-term solution (designated as BACKPR in Table I) with those of our two-term solution as listed in Table I. The values of the drift w and the normalized transverse diffusion coefficient D_TN calculated by the two methods agree to within the estimated numerical accuracy for all E/N. This agreement is expected since the

TABLE I. Calculated transport and excitation coefficients for electrons in N_2 using cross sections derived using conventional two-term techniques.

E/N 10^{-21} V m^2	Technique	w^a 10^8 m sec^{-1}	$D_T N^a$ 10^{24} m^{-1} sec^{-1}	$D_L N$ 10^{24} m^{-1} sec^{-1}	$\frac{\alpha}{N}(v=0\rightarrow 1)$ 10^{-20} m^2	$\frac{\alpha}{N}(A^3\Sigma)^b$ 10^{-22} m^2
40	BACKPR[c]	5.62	1.741	0.667[e]	3.06	0.234
	Two term	5.64	1.745	0.875	3.20	d
	Six term	5.56	1.614	1.094	3.14	d
	MC	5.42	1.604			
70	BACKPR	8.61	1.791	0.731[e]	3.31	1.313
	Two term	8.59	1.793	1.098	3.43	1.305
	Six term	8.43	1.624	1.410	3.35	1.833
100	BACKPR	11.24	2.09	1.088[e]	3.12	6.29
	Two term	11.11	2.10	1.320	3.27	6.41
	Six term	10.95	1.941	1.383	3.12	7.68
	MC	10.90	2.01		3.09	7.67
200	BACKPR	18.73	3.45	2.44[e]	1.726	27.6
	Two term	18.67	3.45	2.07	1.760	27.7
	Six term	18.53	3.18	2.23	1.672	28.1
	MC				1.674	27.7

[a]The two- and six-term values of w and $D_T N$ for $E/N \geq 40\times 10^{-21}$ V m^2 are from I and are repeated here for completeness. Note that the calculated values of $D_L N$ are very sensitive to the choice of the energy grid, the details of the integration procedure, etc.

[b]Direct excitation only. Does not include cascading.

[c]This version of the conventional two-term technique of Ref. 4 is described in detail by P. E. Luft, JILA Information Center Report No. 14, University of Colorado, 1975 (unpublished).

[d]Too small for accurate calculations.

[e]Evaluated using Eq. (25).

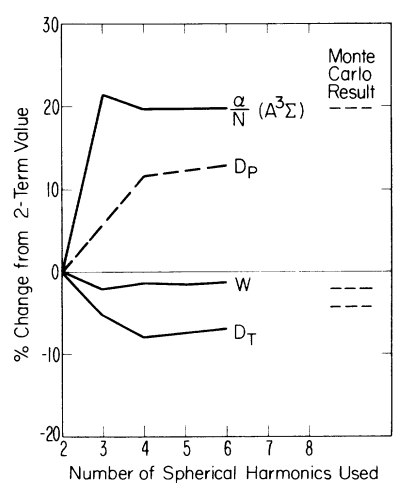

FIG. 4. Convergence of the spherical harmonic expansion results as shown by the change in drift velocity w, transverse D_T and parallel D_L diffusion coefficients, and $A^3\Sigma$ excitation coefficient α/N with the number of spherical harmonics used in the calculation. The dashed lines show the results of the Monte Carlo calculations. Here $E/N=10^{-19}$ V m^2 for N_2.

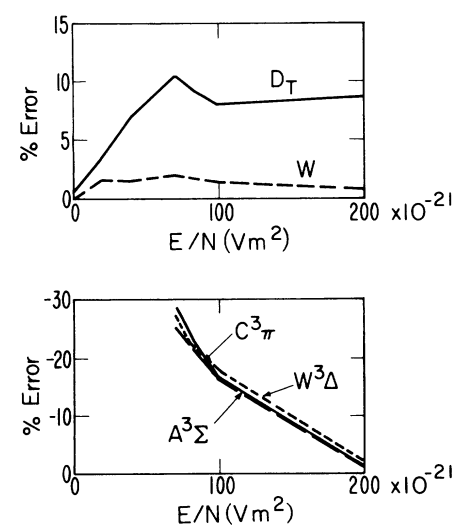

FIG. 5. Error introduced by the two-term approximation when compared to the six-term solutions for drift velocity, transverse diffusion, and certain electronic excitation rates as functions of E/N. The upper part shows the drift velocity w and transverse diffusion coefficient D_T, while the lower part shows the excitation coefficients.

elastic- and inelastic-scattering cross sections are assumed isotropic, since $Q_m(\epsilon)$ is the same for both calculations, and since the last term of Eq. (12) makes a very small contribution to the electron energy losses. In the case of the longitudinal diffusion coefficients listed in Table I we see a significant difference between the results of the conventional two-term solution (BACKPR) and those of our two-term solution. This difference in $D_L N$ is largest at E/N for which the difference between the two-term and six-term results for the other transport coefficients is largest. We therefore attribute the difference to the omission of the $wf_1(\epsilon)$ term in the solution of the $j=1$ equation of Eqs. (12) and in the evaluation of $D_L^{\mathrm{II}}N$ using Eq. (25) in the case of the conventional two-term solution.

Attempts to correlate the difference between the two-term calculation and the multiterm calculation with an energy-loss parameter defined by experiment have been only partially successful. Figure 6 shows the fractional error in the two-term transverse diffusion coefficient as a function of the ratio of the momentum transfer collision frequency to the energy exchange collision frequency,[4] i.e., a measure of the energy-loss per collision. This ratio is also very nearly equal to the ratio of the drift or directed energy to the random energy.[4] When this number is large, the spherical harmonic representation of the distribution function converges slowly and we would expect the two-term approximation to introduce significant error. The points for CH_4 and the ramp model atom are taken from I. About all that can be said from this plot is that the error is equal to or larger than the energy-loss-per-collision parameter. Lin, Robson, and Mason[15] give an estimate of the error in the transverse diffusion coefficient that falls below the straight line of Fig. 6 by about a factor of 2. Their estimate for the error in the drift velocity is more difficult to evaluate but appears to pass through the rather scattered results for N_2, CH_4, and the ramp model atom.

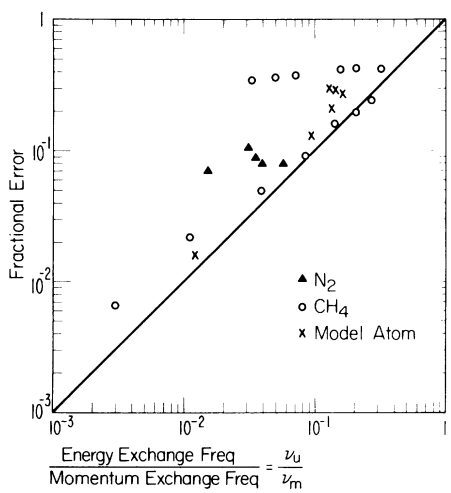

FIG. 6. Error in two-term calculation of transverse diffusion coefficient vs ratio of energy exchange frequency ν_u to momentum exchange frequency ν_m. The solid line assumes that the error in D_T is equal to ν_u/ν_m. The points show the results of I, i.e., ▲: N_2, ○: CH_4, and ×: model atom. Note that for CH_4 and the model atom the error increases with E/N and ν_u/ν_m until ν_u/ν_m reaches a maximum. At higher E/N for CH_4, the error is almost independent of ν_u/ν_m.

IV. ANALYTIC SOLUTION FOR HIGH ENERGIES

In this section we will make use of an analytic solution to Eq. (7) which is valid at high electron energies and low E/N in order to illustrate the nature of the convergence of the spherical harmonic expansion represented by Eq. (10). Long[29] has obtained a steady-state spatially independent solution of Eq. (7) for a uniform electric field and isotropic scattering. He finds that when the third and fourth term on the right-hand side of Eq. (12) are small, ϵ is above the excitation threshold and θ is not near 90° the angular dependent distribution function is given by

$$f(\vec{v})=\frac{Q_e}{Q}\frac{\exp(-\epsilon/kT_f)}{(1-\alpha\cos\theta)}\ , \tag{26}$$

where

$$\alpha=\frac{Q_e}{2Q}\ln\left[\frac{1+\alpha}{1-\alpha}\right]\ , \tag{27}$$

$Q=Q_e+Q_h$, and $kT_f=eE/\alpha NQ$. Here Q_e is the cross section for elastic scattering which is assumed independent of electron energy. $Q_h(\epsilon)$ is the inelastic cross section which is independent of energy for energies above the threshold energy at ϵ_h, i.e., $Q_h(\epsilon)$ is a step function. For $Q_h/Q_e << 1$, $kT_f \rightarrow eE/N(3Q_hQ)^{1/2}$, and $f(\vec{v})$ is well represented by the first two terms of the spherical harmonic expansion. For $Q_h/Q_e >> 1$, $\alpha \rightarrow 1$ so that $kT_f=eE/NQ$ and $f(\vec{v})$ approaches a delta function in the direction of electron acceleration.

We have chosen to make our comparison of the predictions of Eq. (26) with those of Sec. II, for the

moderately severe case of $Q_h = Q_e$, for which $\alpha = 0.9575$. When the θ-dependent portion of Eq. (26) for this case is resolved into spherical harmonics, the relative values of $f_j(\epsilon)/f_0(\epsilon)$ are as shown by the points in Fig. 7. Note that although the ratios of $f_j(\epsilon)$ to $f_0(\epsilon)$ increase with j at low values of j, the ratios are well below the δ-function[20] limit of $(2j+1)$. For higher j the ratios decrease with increasing j in a regular fashion.

The techniques of Sec. II have also been used to calculate the $f_j(\epsilon)$ for the problem of a step-function inelastic cross section with $Q_e = Q_h$. Calculations were made for small enough E/N, i.e., $eE/NQ\epsilon_h = 0.25$, so that $f_0(\epsilon+\epsilon_h) << f_0(\epsilon)$ as required for comparison with Long's model.[30] We find that for $\epsilon/\epsilon_h > 1.5$ the $f_j(\epsilon)$ vary exponentially with ϵ with an effective value of kT_f which is within 10% of that predicted by Eq. (26). The lines of Fig. 7 show the values of $f_j(\epsilon)/f_0(\epsilon)$ vs j calculated using Eqs. (11) for various n and for $\epsilon/\epsilon_h = 1.8$. We see that as n is increased from 2 to 8 the $f_j(\epsilon)/f_0(\epsilon)$ ratios for the lower-j values rapidly converge and approach the limiting values given by Long. As j increases the calculated ratios vary somewhat with ϵ and the values shown are only representative. As an illustration of the convergence of $f_1(\epsilon)$ and $f_0(\epsilon)$ in this case, we note that the calculated electron-drift velocity decreases by 6% as n increases from 2 to 4, but varies by less than 0.2% for $n = 4$, 6, and 8. We consider

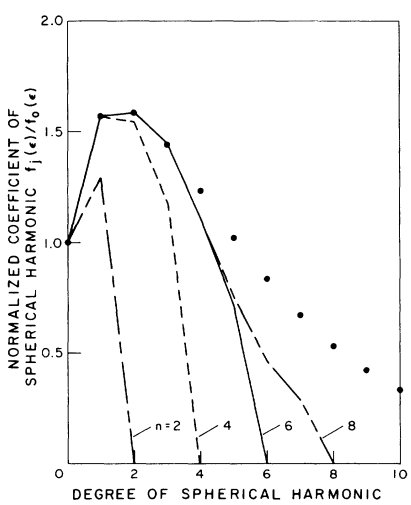

FIG. 7. Comparison of normalized magnitudes of coefficients of spherical harmonics for a step-function model atom as calculated using the procedures of Sec. II and as calculated by Long. The points show values calculated from Long's solution while the lines show results from Sec. III.

the differences in the ratios of $f_j(\epsilon)/f_0(\epsilon)$ and in the kT_f values to be reasonable in view of the differences in the models.[30] The similarities of the results of the two calculations add a measure of confidence to the procedures of Sec. II at energies where the inelastic cross section is large.

As a further example of the similarities of the solutions given by the techniques of Sec. II and that given by Eq. (26), we will compare the predicted effective temperatures T_f for electrons in N_2 with values obtained from the results summarized in Sec. III. For convenience, we have taken into account the dependence of T_f on E/N by examining the quantity $(E/N)/(kT_f)$, which we will call an effective cross section Q_f. According to Eqs. (26) and (27) the value of the effective cross section in the limit of small Q_h/Q_e is given by

$$Q_f = \left[3Q_m^s(\epsilon)\sum Q_0^k(\epsilon)\right]^{1/2} .$$

Here we have taken

$$Q = Q_m^s(\epsilon) = Q_T(\epsilon)$$

and

$$Q_h(\epsilon) = \sum Q_0^k(\epsilon) ,$$

i.e., the scattering is assumed to be isotropic, and have allowed Q_f to vary with electron energy. The values of $Q_f(\epsilon)$ in this limit are calculated from the data of Fig. 1 and are shown as a function of ϵ by the solid curve of Fig. 8. In the limit of large Q_h/Q_e, we have used $Q_f = Q_m^s(\epsilon) = Q_T(\epsilon)$, and have shown the results as the dashed curve of Fig. 8. The results of Sec. III are used to obtain values of $(kT_f)^{-1} \equiv -d\ln f_0(\epsilon)/d\epsilon$ and the values of $(E/N)/(kT_f)$ are shown as the points in Fig. 8 for three different values of E/N. The points are close to the solid curve when $(\epsilon_h/f_0)\,|\,df_0/d\epsilon\,|$ is large. Here ϵ_h is a typical excitation threshold energy, i.e., $\epsilon_h \sim 8$ eV for $\epsilon > 10$ eV and $\epsilon_h \sim 0.3$ eV for $\epsilon \sim 2$ eV. Except near 5 eV and below 2 eV, the agreement of the effective cross section calculated from the results of Sec. III and from our application of Long's very simple solution is surprisingly good. The success of this comparison suggests to us that Long's formulas could be used to obtain a high-energy boundary condition for the formulas of Sec. II or an initial estimate of the temperature T_b in the high energy or "tail" region of Ref. 15.

V. ELECTRODE EFFECTS

In order to justify the comparison of experimental values of the swarm parameters with those cal-

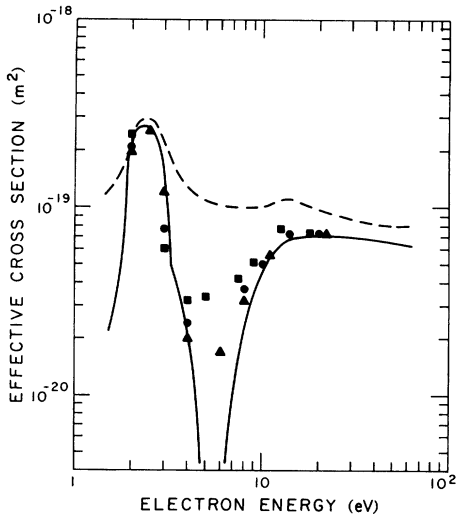

FIG. 8 Comparison of effective cross sections for calculation of apparent electron temperature using Long's formula. The points are determined from the six-term solutions to the electron Boltzmann equation for N_2 given in Sec. III for various E/N. The symbols and E/N are ▲, 4×10^{-20}; ●, 10^{-19}; and ■, 2×10^{-19} $\mathrm{V\,m^2}$. The solid curve shows the effective cross section expected for a small ratio of inelastic to elastic cross section while the dashed curve shows the effective cross section expected for a large ratio of inelastic to elastic cross sections.

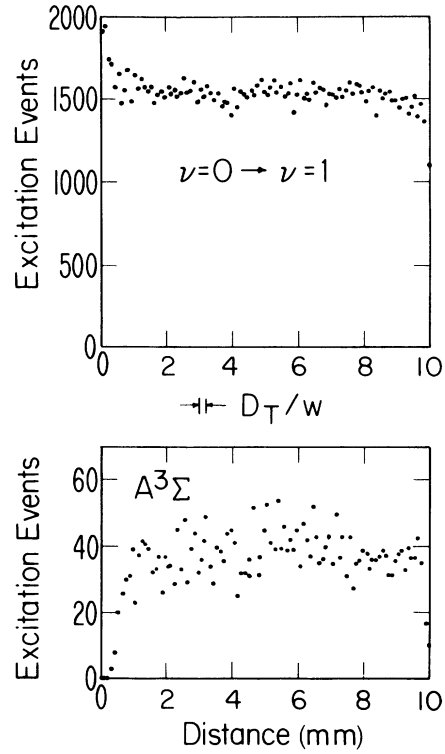

FIG. 9. Monte Carlo calculations of the number of excitation events as a function of distance in a drift region for $v=0\rightarrow1$ vibrational excitation (upper part) and $A\,^3\Sigma$ electronic excitation (lower part). This calculation is for $N=10^{23}$ $\mathrm{m^{-3}}$ and $E/N=10^{-19}$ $\mathrm{V\,m^2}$.

culated, the hydrodynamic model represented by Eqs. (2) and (3) must be shown to accurately model the experimental situation. Thus far, we have applied this model to the calculation of swarm parameters and have determined the approximations that yield converged transport and excitation coefficients. Since the hydrodynamic approach taken here cannot take into account the effect of the electrodes present in experiments, a Monte Carlo simulation was done to determine the effect of the electrodes on the measured values of swarm parameters.

We have performed Monte Carlo calculations in N_2 using the set of cross sections presented in Fig. 1. The simulation conditions of a 10-mm drift distance and a density of 10^{23} $\mathrm{m^{-3}}$ at 10^{-19} $\mathrm{V\,m^2}$ were chosen to approximate the conditions of the measurements[23,24] of excitation coefficients in N_2. For this calculation, single electrons were released normal to the cathode with 2-eV energy. The electrons were allowed to drift through the tube and were absorbed at the cathode and anode. Upon absorption at the cathode, a new electron was released with the same initial conditions. The simulation continued until the electrons encountered 10^6 collisions with the neutrals. A record was kept after each collision of the type of collision and the position of the electron in the drift tube when the collision took place. From this record we have plotted the number of excitation events per distance interval as a function of distance as seen in Fig. 9 for the $v=0\rightarrow1$ and $A\,^3\Sigma$ excitation processes.

The effect of the cathode and anode can be seen in the plots of Fig. 9 as a change in the excitation rates near these electrodes. One can estimate the distance required for the electrons to reach a steady-state energy distribution from the distance which the electrons drift during an energy relaxation time.[4,31] This distance is equal to D_T/w and for the conditions of Fig. 9 is 0.2 mm. This is roughly the distance required for the excitation rates to reach the steady-state values. The $v=0\rightarrow1$ excitation rate starts out higher than the steady-state rate because the release energy of 2 eV is equal to the energy at which the vibrational excitation cross section is a maximum. On the other hand, the $A\,^3\Sigma$-state excitation with a thresh-

old energy of 6.17 eV cannot take place until some electrons have gained enough energy from the field to reach the A-state threshold. These trends in the excitation near the cathode do, of course, depend on the release energy chosen. The anode effects are independent of the release conditions provided a steady-state has been established at some point in the drift region.[32,33] Here again, the electrode effects are found to occur on a scale corresponding to the D_T/w energy relaxation distance.

When the excitation rates calculated from the Monte Carlo simulation for the whole gap are compared with those given in Table I the agreement is good ($<1\%$) for the $v=0\rightarrow 1$ transition and only fair (7% low) for the A-state excitation. However, when excitation events near the boundaries (1 mm on either end) are excluded, the Monte Carlo rates agree with those of Table I to within 0.5%. We conclude from this excellent agreement that the hydrodynamic approximation is valid for the conditions of published N_2 excitation experiments.[23] The most accurate comparisons between the results of the Boltzmann calculations described in this paper and the results of excitation experiments will be for those experiments in which the data are obtained from regions far from the electrodes.

VI. CONCLUSIONS

We have presented a study of the convergence properties of solutions of the electron Boltzmann equations and calculated swarm parameters in the case of N_2 at moderate field strengths $(1-200)\times 10^{-21}$ V m^2. The cross sections used as input to the calculations are taken from previous two-term analyses of electron swarms in N_2. No attempt was made to improve these cross sections or to compare these calculations with experiment but rather these cross sections were used as typical molecular cross sections in order to determine the error introduced in the calculated swarm parameters by the usual approximations. One of the many applications of the two-term approximation has been in the iterative extraction of cross sections from measured swarm parameters by comparison of calculated and experimental values of the swarm parameters. The accuracy of the cross sections thus deduced will of course depend on the accuracy of the calculational method. We find that in the worst cases for N_2 the error introduced by the two-term spherical harmonic approximation is small ($\sim 1\%$) for drift velocities, larger for the diffusion coefficients ($\sim 5\%$), and even larger for the excitation rates (30%). The maximum error in the transport coefficients occurred at an E/N of 70×10^{-21} V m^2, where the mean energy of the electrons is close to the energy for which the ratio of inelastic to elastic cross sections is the largest. Convergence of the transport and excitation coefficients with the number of terms in the expansion to within a few percent was achieved by the use of four spherical harmonic terms in all cases. These errors are significant for the extraction of cross sections from swarm experiments if those cross sections are to be compared, for example, with beam data.

The calculations reported in this paper verify the usual criteria for the application of the two-term approximation to the calculation of electron transport and reaction coefficients, i.e., the requirement that the sum of inelastic cross sections be small compared to the sum of the elastic momentum transfer cross sections. This means that the two-term approximation is valid for many of the gas mixtures used in applications, e.g., the more dilute mixtures of N_2 and CO_2 in He used in CO_2 lasers. However, the errors in the determination of the collision cross sections resulting from the use of the two-term approximation in gases with large inelastic cross sections, e.g., N_2, will lead to errors in the calculated transport coefficients for the dilute mixtures. The magnitude of these errors has yet to be determined. Note that the errors in calculated transport coefficients should be small when two-term-derived cross sections are used with the two-term approximation to interpolate or extrapolate the transport data for a pure or nearly pure gas even though the ratio of the inelastic to elastic cross sections is large.

At the moderate E/N considered in this paper convergence of the transport and rate coefficients is achieved independently of convergence of the distribution function, i.e., the coefficients become independent of the number of spherical harmonics used even though higher-order Legendre expansion coefficients in N_2 are not negligible with respect to the isotropic component. The generality of this observation made for N_2 is in agreement of the results of I and is supported by our comparison of results for a model atom. Even for the moderately extreme case of equal elastic and inelastic cross sections we found good agreement between the results of calculations using the spherical harmonic expansion and the results of the analytic solution for those $f_j(\epsilon)$ of importance in transport and exci-

tation coefficient calculations.

The results of Monte Carlo calculations performed with the same cross sections as the Boltzmann calculations compare very well with the Boltzmann results. The effect of physical boundaries on the measured swarm parameters was investigated using Monte Carlo techniques. The conclusion from that calculation is that an equilibrium is indeed established very quickly on the scale of typical experiments at these values of E/N and the hydrodynamic assumption which is implicit in our Boltzmann formulation is valid.

We conclude that the Boltzmann formulation presented here to describe the motion of the electron swarm in N_2 at moderate E/N is an adequate model of the experiment. It remains to be seen just how high the E/N values can be before our formulation begins to fail. For example, at E/N values higher than those considered here, it is necessary to treat the effect of new electrons due to ionization. We are now looking at the problem of electron swarms in N_2 at high values of E/N.

ACKNOWLEDGMENTS

The authors would like to acknowledge numerous helpful discussions of the problem of solutions to the Boltzmann equation with W. P. Allis. We would also like to thank H. R. Skullerud for providing the details of the formulation of the density-gradient expansion, S. V. ONeil for timely help with this problem, and W. H. Long, Jr. for permission to quote his results prior to publication. The authors would like to acknowledge a computer grant from the National Center for Atmospheric Research, Boulder, Colorado. This work was supported in part by Wright-Patterson Air Force Base under MIPR No. FY1455-80-00608.

---

*Current address: Sandia National Laboratories, Division 4211, Albuquerque, New Mexico 87185.

†Quantum Physics Division, National Bureau of Standard and Department of Physics, University of Colorado, Boulder, Colorado 80309.

[1]L. C. Pitchford, S. V. ONeil, and J. R. Rumble, Jr., Phys. Rev. A 23, 294 (1981).

[2]T. Holstein, Phys. Rev. 70, 367 (1946).

[3]W. P. Allis, *Handbuch der Physik*, edited by S. Flügge (Springer, Berlin, 1956), Vol. 21, p. 383; I. P. Shkarofsky, T. W. Johnston, and M. P. Bachynski, *The Particle Kinetics of Plasmas* (Addison-Wesley, Reading, Mass., 1966), Chap. 3; L. G. H. Huxley and R. W. Crompton, *The Diffusion and Drift of Electrons in Gases* (Wiley, New York, 1974), Chap. 2.

[4]L. S. Frost and A. V. Phelps, Phys. Rev. 127, 1621 (1962); A. G. Engelhardt, A. V. Phelps, and C. G. Risk, Phys. Rev. 135, A1566 (1964).

[5]J. J. Lowke and J. H. Parker, Jr., Phys. Rev. 181, 302 (1969).

[6]W. L. Nighan, Phys. Rev. A 2, 1989 (1970).

[7]R. Winkler and S. Pfau, Beitr. Plasmaphys. 13, 273 (1973); 14, 169 (1974); S. Pfau and R. Winkler, *ibid.* 18, 113 (1978); V. V. Starykh, J. Wilhelm, and R. Winkler, *ibid.* 20, 2 (1980).

[8]T. Taniguchi, H. Tagashira, and Y. Sakai, J. Phys. D 11, 1757 (1978); H. Tagashira, T. Taniguchi, and Y. Sakai, *ibid.* 13, 235 (1980).

[9]R. A. Latypova, A. I. Lukovnikov, and E. P. Fetisov, Zh. Tekh. Fiz. 42, 115 (1972) [Sov. Phys.—Tech. Phys. 17, 88 (1972)]; A. Kh. Mnatsakanyan and G. V. Naidis, Fiz. Plazmy. 2, 152 (1976) [Sov. J. Plasma Phys. 5, 84 (1976)]; N. L. Aleksandrov, A. M. Konchakov, and É. E. Son, Fiz. Plazmy. 4, 169 (1978); 4, 1182 (1978) [Sov. J. Plasma Phys. 4, 98 (1978); 4, 663 (1978)]; Teplofiz. Vys. Temp. 17, 210 (1979) [High Temp. (USSR) 17, 179 (1979)]; É. E. Son, *ibid.* 16, 1162 (1978) [16, 990 (1978)]; S. V. Nikonov, A. P. Osipov, and A. T. Rakhimov, Kvant. Elektron. (Moscow) 6, 1258 (1979) [Sov. J. Quantum Electron. 9, 740 (1979)]; V. A. Pivovar and T. D. Sidorova, Zh. Tekh. Fiz. 49, 1436 (1979) [Sov. Phys.—Tech. Phys. 24, 799 (1979)]; K. Rohlena and T. Ruzicka, Czech. J. Phys. B29, 407 (1979).

[10]L. A. Newman and T. A. DeTemple, J. Appl. Phys. 47, 1912 (1976); O. Judd, IEEE J. Quantum Electron. QE-12, 78 (1976); G. R. Govinda Raju and G. R. Gurumurthy, Int. J. Electron. 4, 355 (1978); H. Brunet and P. Vincent, J. Appl. Phys. 50, 4708 (1979).

[11]G. J. Schulz, Phys. Rev. 125, 229 (1962); 135, A988 (1964).

[12]W. H. Long and W. F. Bailey, Bull. Am. Phys. Soc. II 19, 151 (1974). Momentum transfer cross sections for inelastic collisions in N_2 have been evaluated from experiment by D. C. Cartwright, J. Appl. Phys. 49, 3855 (1978).

[13]L. E. Kline and J. G. Siambis, Phys. Rev. A 5, 794 (1972); L. Friedland, Phys. Fluids 20, 1461 (1972). See also H. N. Kücüparpaci and J. Lucas, J. Phys. D 12, 2123 (1979).

[14]P. Kleban and H. T. Davis, J. Chem. Phys. 68, 2999 (1978).

[15]S. L. Lin, R. E. Robson, and E. A. Mason, J. Chem. Phys. 71, 3483 (1979).

[16]I. D. Reid, Aust. J. Phys. 32, 231 (1979).

[17]K. Kumar, H. R. Skullerud, and R. E. Robson, Aust. J. Phys. 33, 343 (1980). In the notation of these authors, $w=\omega^{(1)}$, $D_T=\omega^{(2x)}$, and $D_L=\omega^{(2z)}$.

[18]For various recent approaches yielding essentially the same result for the effects of spatial gradients see, J. H. Parker, Jr. and J. J. Lowke, Phys. Rev. 181, 290 (1969); H. R. Skullerud, J. Phys. B 2, 696 (1969); H. R. Skullerud, Aust. J. Phys. 27, 195 (1974); H. Tagashira, Y. Sakai, and S. Sakamoto, J. Phys. D 10, 1051 (1977).

[19]Note that the sign of the third term on the right-hand side of Eq. (7) of I is in error. Also note that in the present paper we have chosen to measure θ from the direction of electron acceleration rather than from the direction of the electric-field vector as in I. This changes the sign of each of the terms containing E in Eq. (7) of I. Finally, in this paper ϵ replaces $e\epsilon$ in paper I.

[20]When the set of energy grid points were chosen to take into account structure in the excitation cross sections and to yield sufficiently small $f_j(\epsilon_{\max})$, the solutions of Eqs. (11) were found to be insensitive to the choice of $\epsilon_{\max}$ and to the imposition of addition constraints on the $f_j(\epsilon)$. For example, when our numerical calculations and theoretical calculations by Allis (private communication) suggested that $f_j(0)=0$ for $j\geq 1$ and realistic inelastic cross sections, we carried out calculations in which this condition was imposed on the $f_j(\epsilon)$. The changes in the $f_0(\epsilon)$ and the transport and excitation coefficients were small enough to be neglected. In addition to variations in the constraints on the $f_j(\epsilon)$ for $j\leq n-1$, we also tried the "maximum-anisotropy" condition for the truncation of the spherical harmonic coefficients, i.e., instead of $f_n(\epsilon_{\max})=0$ we used $f_n(\epsilon_{\max})=(2n+1)f_{n-1}(\epsilon_{\max})/(2n-1)$ as suggested by G. A. Baraff, Phys. Rev. 133, A26 (1964). We found that this truncation produced changes in $f_j(\epsilon)$ near $\epsilon=0$, but produced little change in the calculated transport and excitation coefficients.

[21]As for the $f_j(\epsilon)$ functions, the several different sets of boundary conditions for $G_j(\epsilon)$ and $H_j(\epsilon)$ produced negligible differences in the calculated diffusion coefficients. The condition on $H_0(\epsilon)$ is discussed immediately after Eq. (16).

[22]The relation

$$\int P_j^1(\cos\theta')I(\epsilon,\theta_s)d\Omega=P_j^1(\cos\theta)\int P_j(\cos\theta_s)I(\epsilon,\theta_s)d\Omega$$

was used to reduce the collision term to the same form as Eq. (12). Here $\cos\theta'=\cos\theta\cos\theta_s$, where θ' and θ are the polar angles before and after scattering through an angle of θ_s. Also, Ω is the solid angle.

[23]W. Legler, Z. Phys. 173, 169 (1963); D. Levron and A. V. Phelps, Bull. Am. Phys. Soc. 24, 129 (1979); V. V. Urosević, Z. Lj. Petrović, J. V. Bozin, and Lj. D. Zeković, *Proceedings of the Symposium on the Physics of Ionized Gases,* edited by Cobić (Boris Kidrić Institute, Beograd, 1980), p. 88.

[24]K. Tachibana and A. V. Phelps, J. Chem. Phys. 71, 3544 (1979).

[25]G. A. Baraff and S. J. Buchsbaum, Phys. Rev. 130, 1007 (1963).

[26]For a discussion of this approximation, see R. D. Hake, Jr. and A. V. Phelps, Phys. Rev. 158, 70 (1967).

[27]Although it does not seem to change the behavior of the higher-energy electrons significantly, we find this low-energy discrepancy to be very prevalent. The shape of the distribution does not change significantly with the time step or total number of collisions used in our Monte Carlo calculation. Using the techniques of I and our Sec. II, we find that the discrepancy occurs with the ramp model atom and CH_4 cross-section sets of I and at all E/N tested for N_2. This discrepancy is also present in calculations using several other Monte Carlo and Boltzmann codes. See A. I. McIntosh, Aust. J. Phys. 27, 59 (1974); Y. Sakai, H. Tagashira, and S. Sakamoto, J. Phys. D 10, 1035 (1977). As in the latter reference we also find a disturbing minimum near 90° in the angular distributions calculated using the Monte Carlo code. As examples of the effect these differences in the distribution can have on calculated rate coefficients for low-energy collision processes, we note that rate coefficients calculated using the two distributions of Fig. 3 for electrons which are either recombining with H_3O^+ or attaching to SF_6 typically differ by 30%. The cross sections for electron-ion recombination with H_2O^+ are from R. A. Heppner, F. L. Walls, W. T. Armstrong, and G. H. Dunn. Phys. Rev. A 13, 1000 (1976), while those for electron attachment to SF_6 are from L. E. Kline, D. K. Davies, C. L. Chen, and P. J. Chantry, J. Appl. Phys. 50, 6789 (1979). A Monte Carlo calculation which apparently does not show the low values of $f_0(\epsilon)$ at low ϵ is that of Friedland (Ref. 13).

[28]Our result that for N_2 the Monte Carlo calculation yields higher rates of electronic excitation than does the two-term calculation is the opposite of that found for CO_2:N_2:He mixtures by G. L. Braglia, R. Bruzzes, and G. L. Caraffini, Lett. Nuovo Cimento 25, 139 (1979).

[29]W. H. Long, Jr., Air Force Aero Propulsion Laboratory Report No. AFAPL-TR-79-2038 (unpublished).

[30]This condition is necessary since Long's model neglects the inelastically scattered electron, whereas according to our calculations, this electron reenters the distribution with a loss of energy equal to ϵ_h. The restriction on the values of θ for which Eq. (26) ap-

plies, arises from Long's neglect of angular dependent terms on the left-hand side of Eq. (7).

[31]See also, J. J. Lowke and D. K. Davies, J. Appl. Phys. 48, 4991 (1977).

[32]J. H. Whealton, D. S. Burch, and A. V. Phelps, Phys. Rev. A 15, 1685 (1977).

[33]H. A. Blevin, J. Fletcher, and S. R. Hunter, J. Phys. D 11, 1653 (1978); Aust. J. Phys. 31, 299 (1978).